

Figure S1 A-F

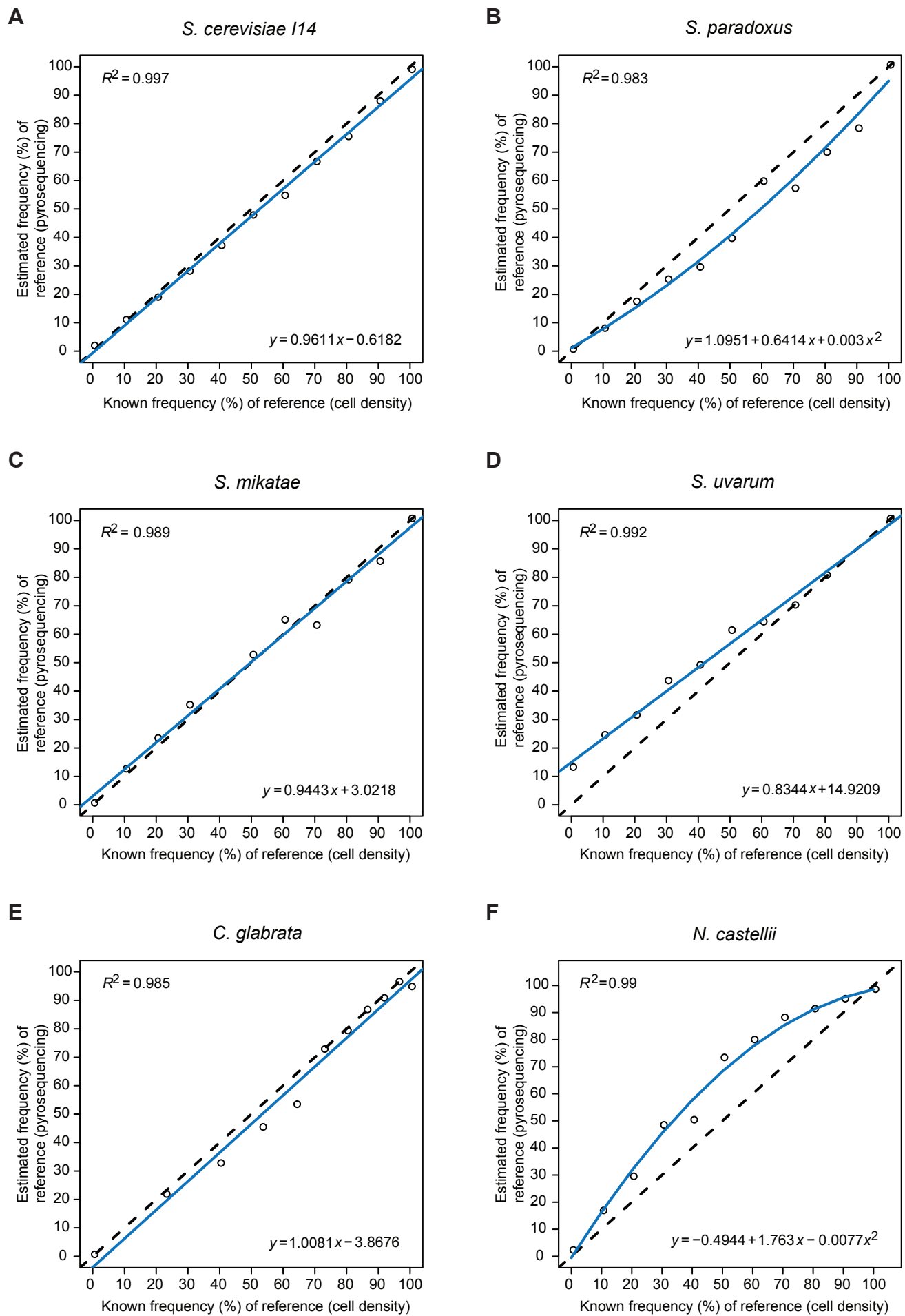
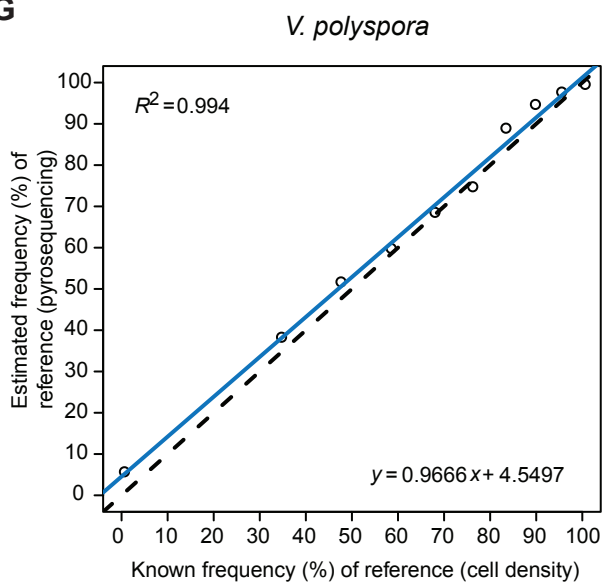
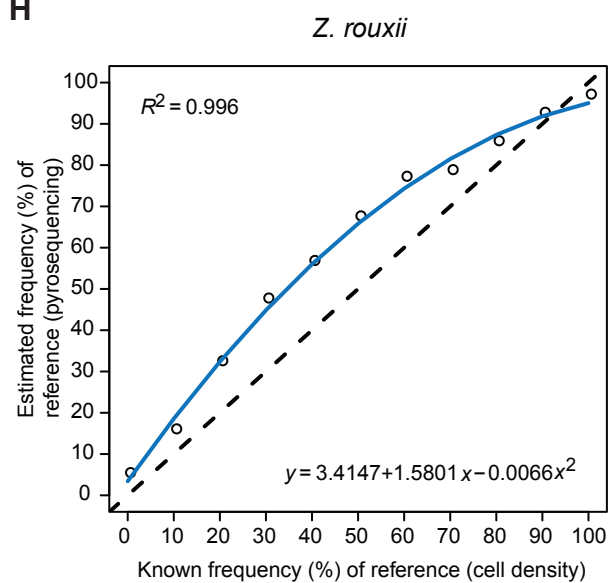


Figure S1 G-L

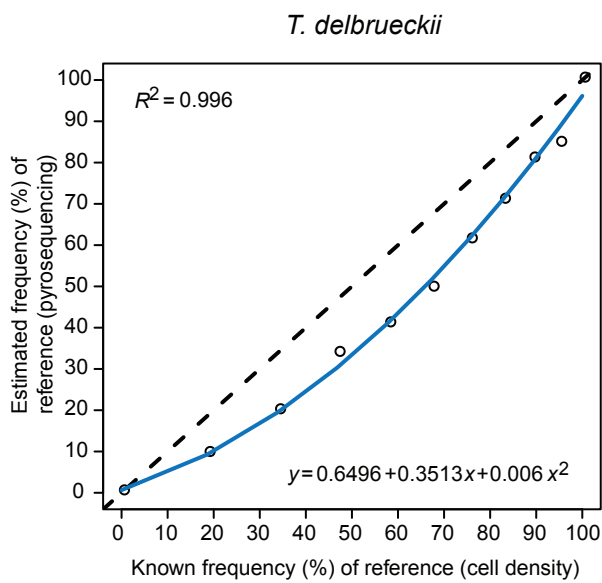
G



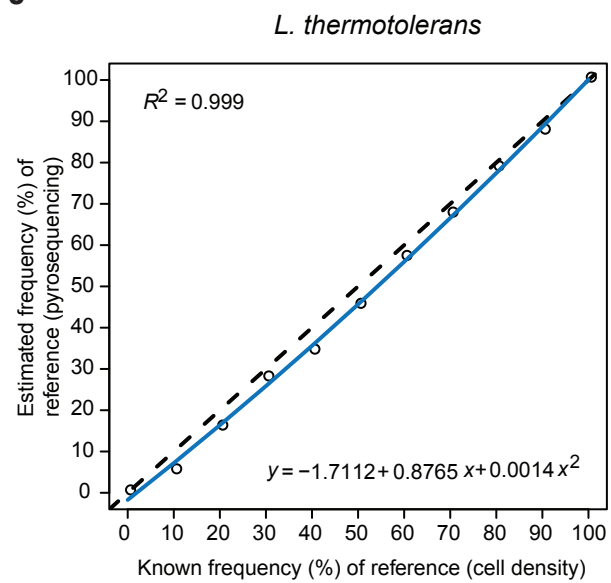
H



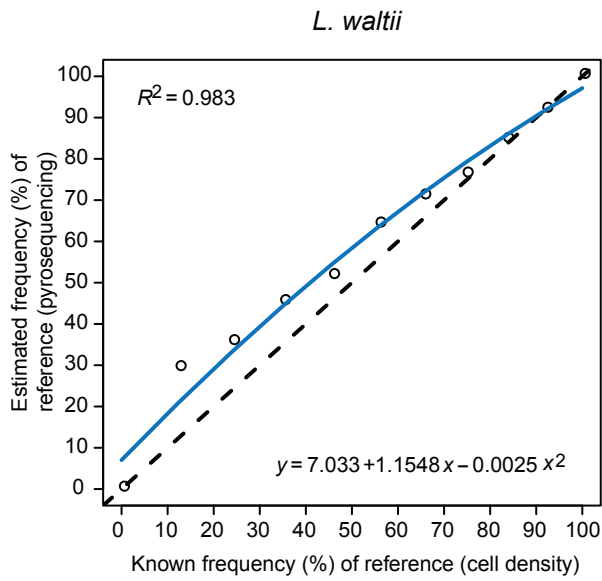
I



J



K



L

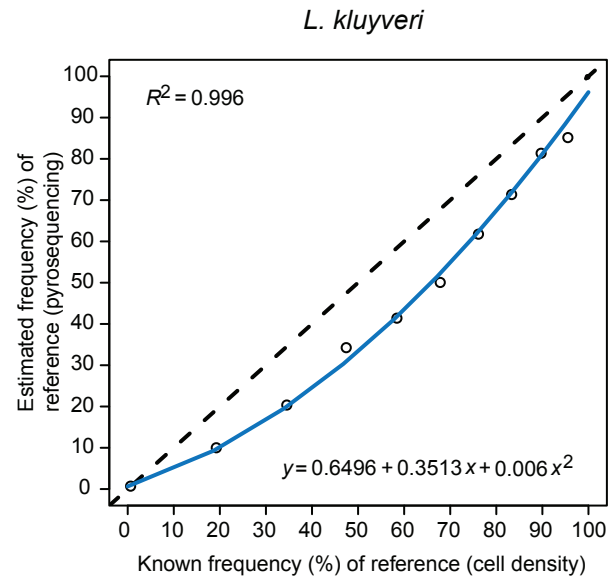


Figure S1 M

M

H. vineae

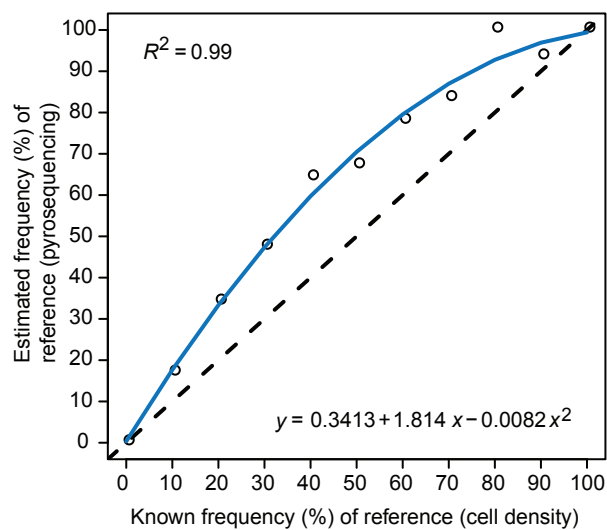
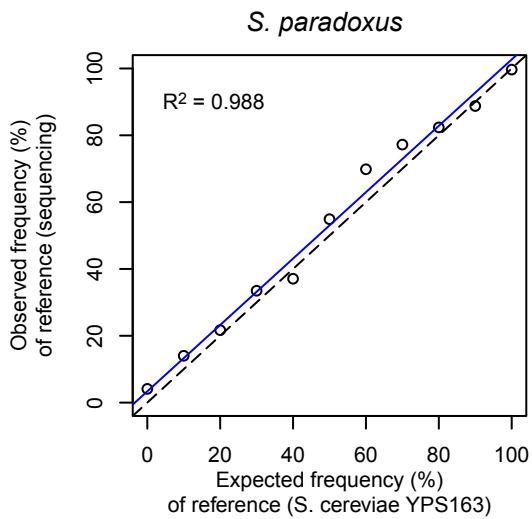


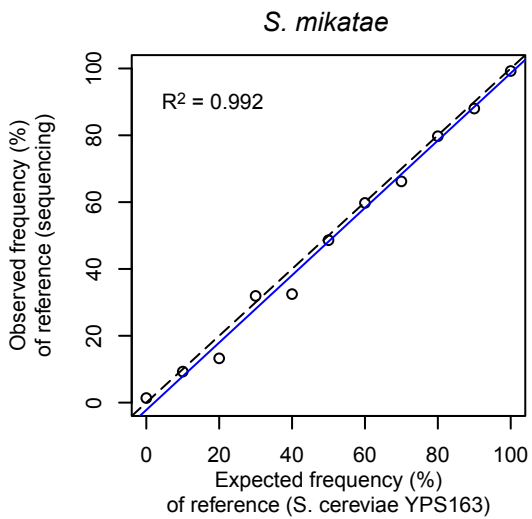
Figure S1. Pyrosequencing calibration. Relationship between the known frequency (%) of the reference species based on cell density and the estimated frequency (%) of the reference species based on pyrosequencing relative to *S. cerevisiae* (YPS163). Reference species are *S. cerevisiae* (I14) (A), *S. paradoxus* (B), *S. mikatae* (C), *S. uvarum* (D), *C. glabrata* (E), *N. castellii* (F), *V. polyspora* (G), *Z. rouxii* (H), *T. delbrueckii* (I), *L. thermotolerans* (J), *L. waltii* (K), *L. kluyveri* (L), and *H. vineae* (M). Calibration equations based on linear or polynormal regression analysis and R-squared values for each model are shown.

Figure S2 A-F

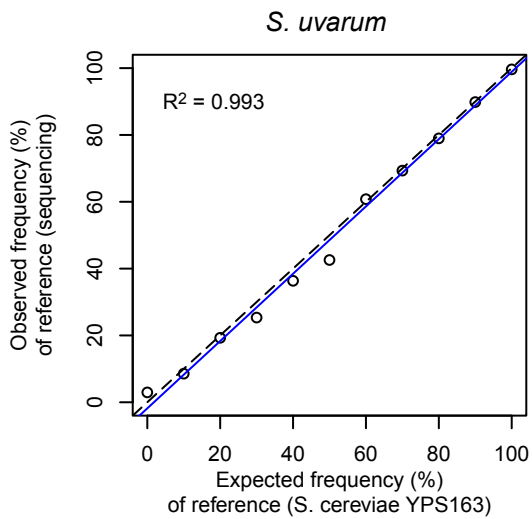
A



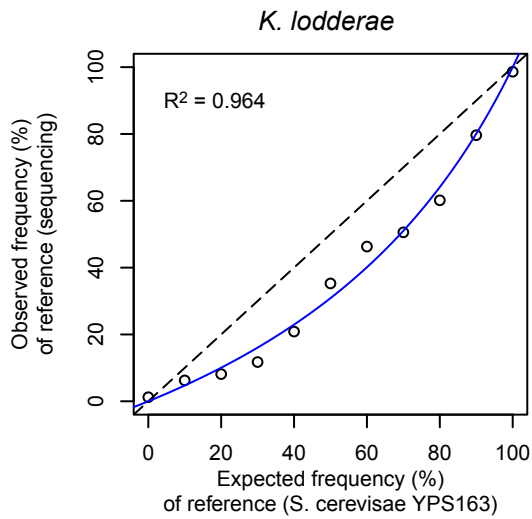
B



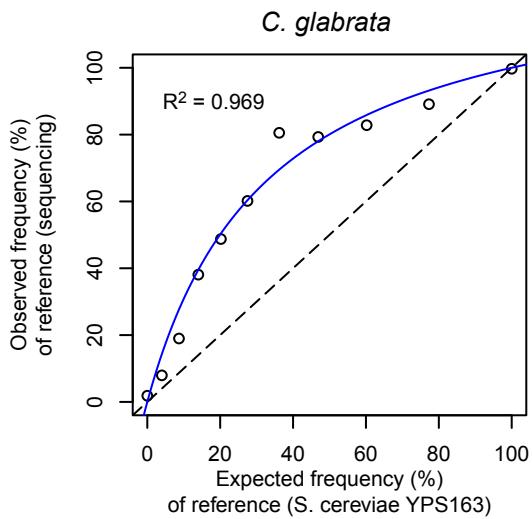
C



D



E



F

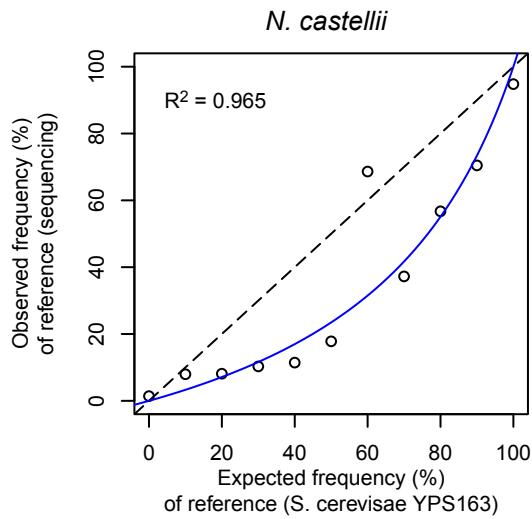


Figure S2 G-K

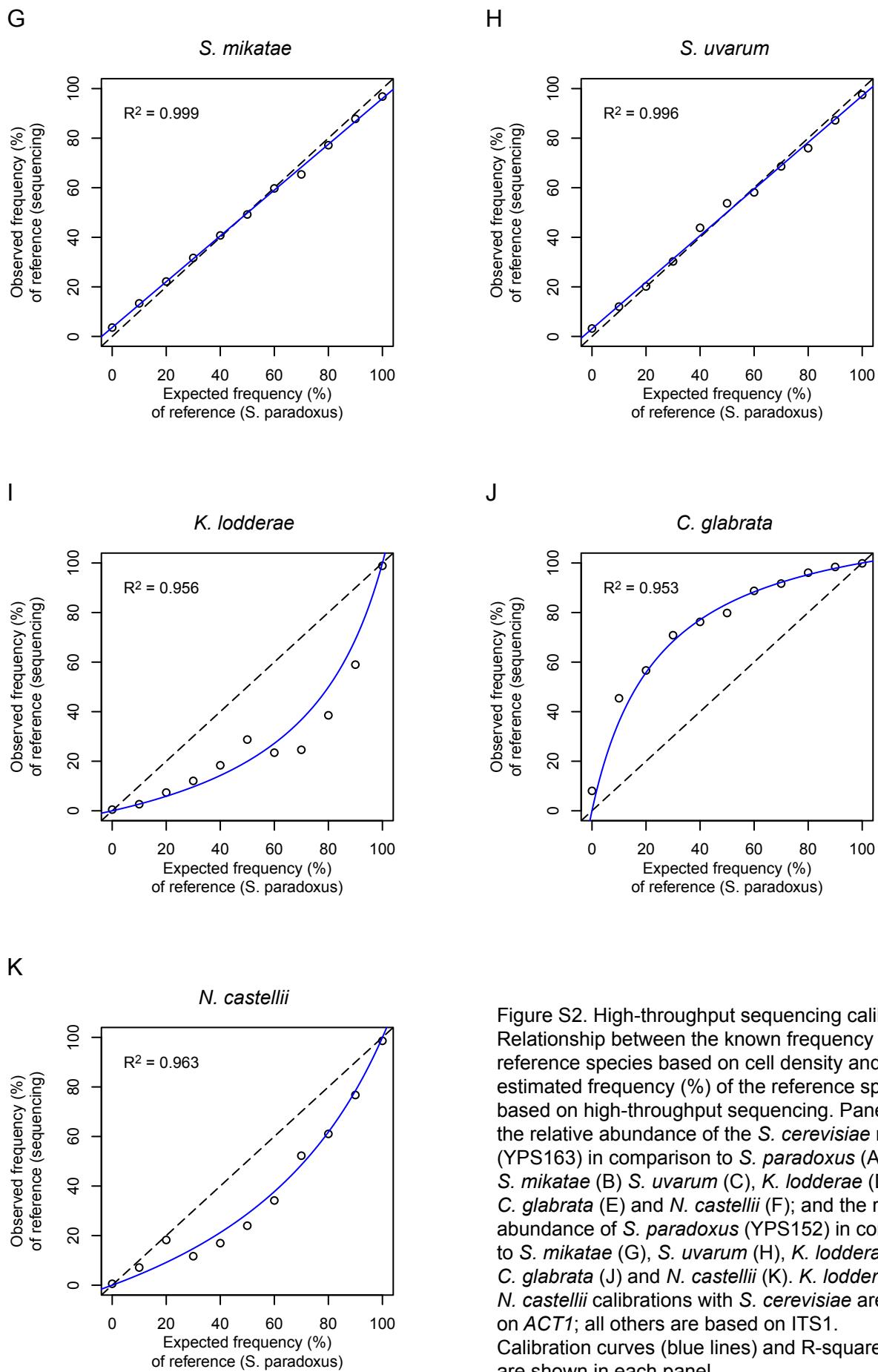


Figure S2. High-throughput sequencing calibration. Relationship between the known frequency (%) of the reference species based on cell density and the estimated frequency (%) of the reference species based on high-throughput sequencing. Panels show the relative abundance of the *S. cerevisiae* reference (YPS163) in comparison to *S. paradoxus* (A), *S. mikatae* (B) *S. uvarum* (C), *K. lodderae* (D), *C. glabrata* (E) and *N. castellii* (F); and the relative abundance of *S. paradoxus* (YPS152) in comparison to *S. mikatae* (G), *S. uvarum* (H), *K. lodderae* (I), *C. glabrata* (J) and *N. castellii* (K). *K. lodderae* and *N. castellii* calibrations with *S. cerevisiae* are based on ACT1; all others are based on ITS1. Calibration curves (blue lines) and R-squared values are shown in each panel.

Figure S3

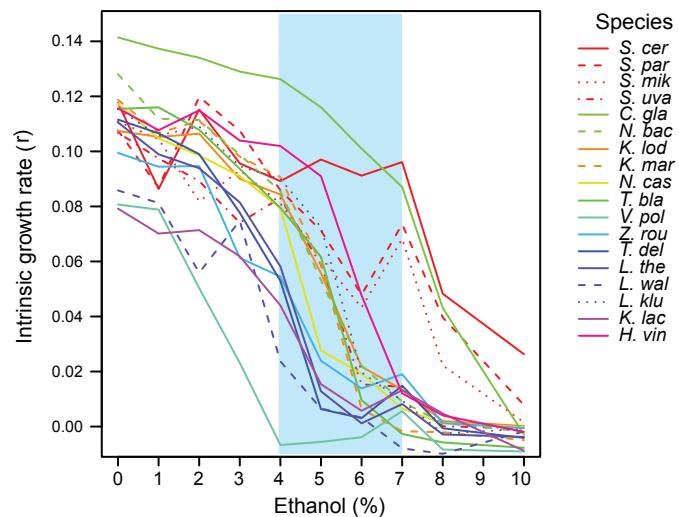


Figure S3. The effect of ethanol on the intrinsic growth rate of each species. Each line shows mean intrinsic growth rate (r) of an individual species based on three replicates as a function of ethanol (%) added at the beginning of growth. Significant differences in the growth rate of each species and *S. cerevisiae* are shown for FDR < 0.01 (shaded region). Error bars have been omitted for clarity.

Figure S4 A-I

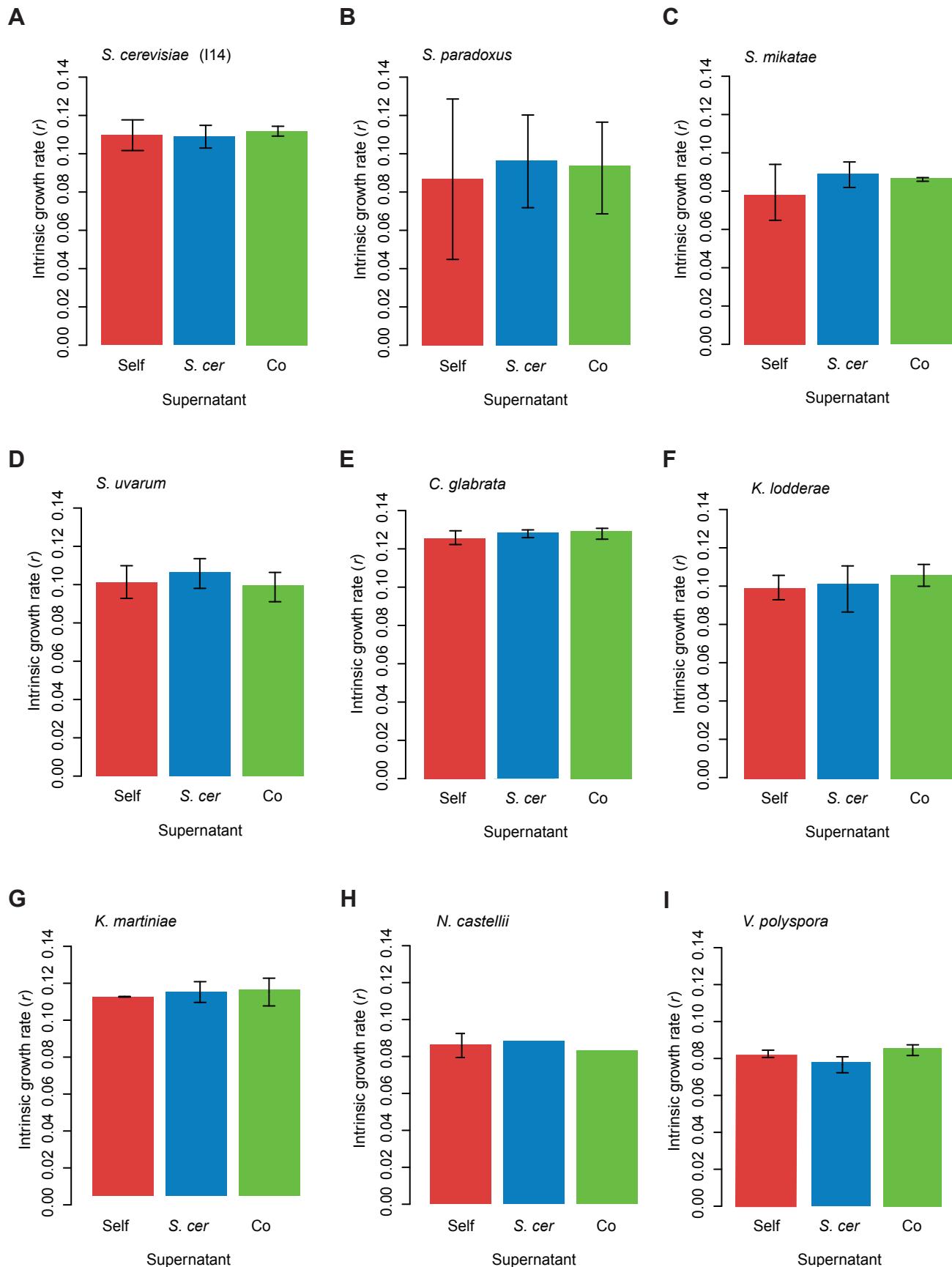


Figure S4 J-O

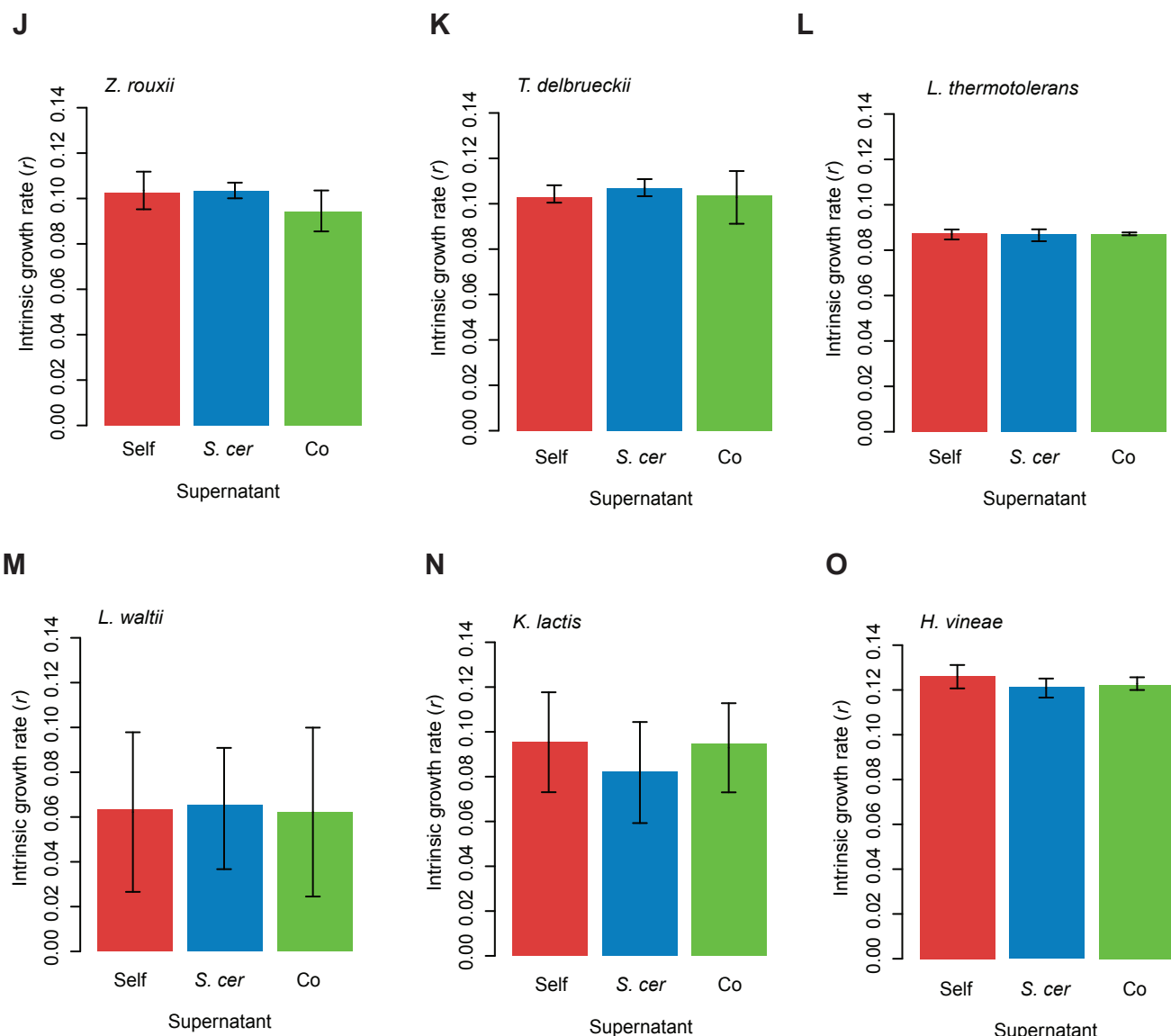
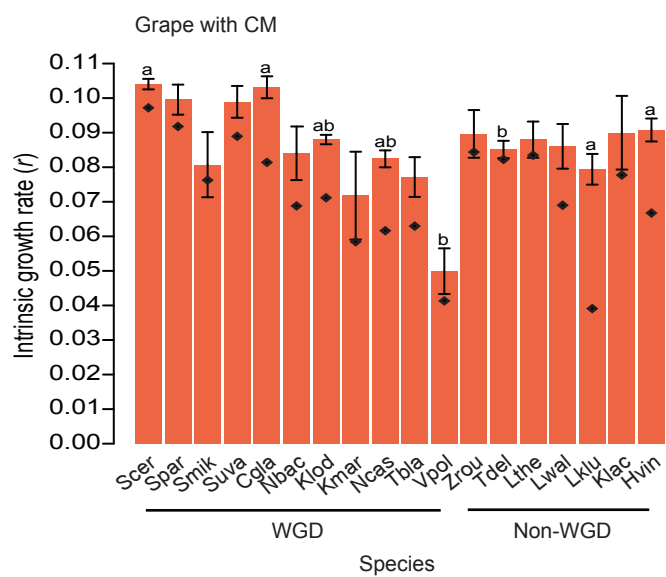


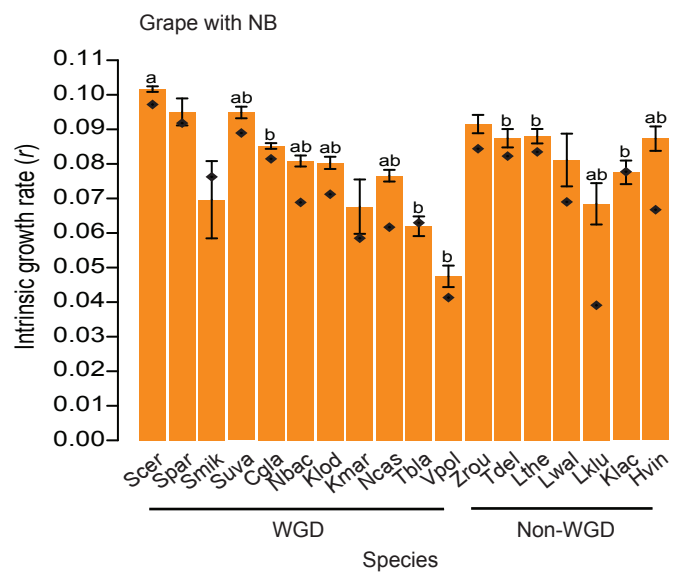
Figure S4. Intrinsic growth rate in YPD made with supernatant. The intrinsic growth rate of each species (A-O) in YPD made with the supernatant from each species' own supernatant when grown in mono-culture (red), the supernatant from *S. cerevisiae* (YPS163) grown in mono-culture (blue), and the supernatant from co-culture with *S. cerevisiae* (green). Species are *S. cerevisiae* (A), *S. paradoxus* (B), *S. mikatae* (C), *S. uvarum* (D), *K. loddetiae* (F), *N. castellii* (G), *C. glabrata* (H), *V. polyspora* (I), *Z. rouxii* (J), *T. delbrueckii* (K), *L. thermotolerans* (L), *L. waltii* (M), *K. lactis* (N), and *H. vineae* (O). Bars and whiskers represent the mean and standard deviation of the growth rate.

Figure S5

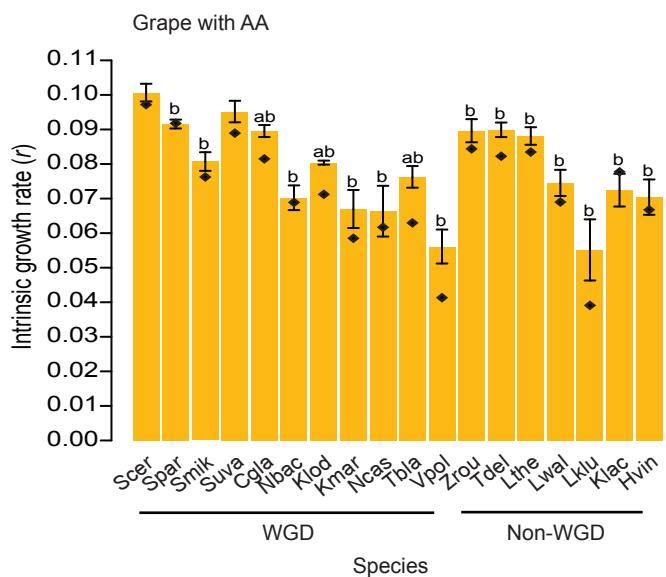
A



B



C



D

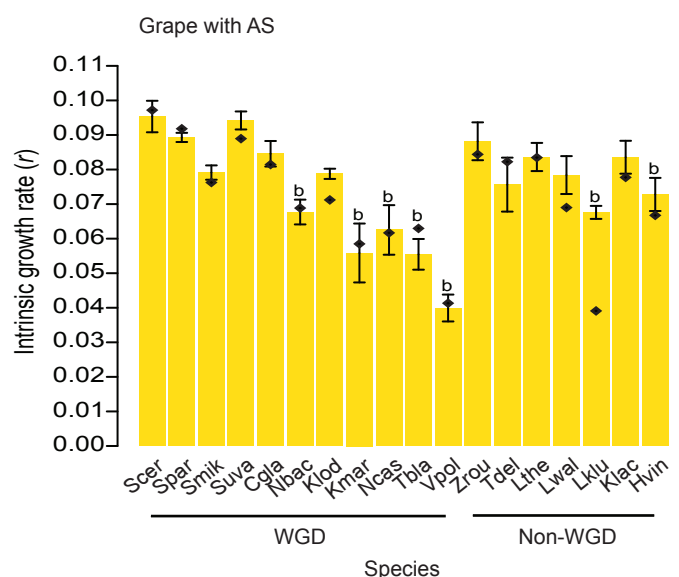


Figure S5. Intrinsic growth rate in Grape supplemented with various nutrients. The mean intrinsic growth rate of each species in Grape supplemented with CM (A), NB (B), AA (C) and AS (D). WGD and non-WGD species are indicated. Bars and whiskers represent the mean and standard deviation of the growth rate. Diamonds represent the average growth rate in Grape without supplements. Significant differences in the growth rate of each species with or without the added nutrient (a) and differences between *S. cerevisiae* and each species with the added nutrient (b) are labeled above each bar for FDR < 0.01.